Calorimetry

Peter Križan

- Basic principles
- Interaction of charged particles and photons
- Electromagnetic cascades
- Nuclear interactions
- Hadronic cascades
- Homogeneous calorimeters
- Sampling calorimeters

Calorimetry:

Energy measurement by total absorption, combined with spatial reconstruction.

Calorimetry is a “destructive” method

Detector response α E

Calorimetry works both for

- charged (e± and hadrons) and
- neutral particles (n,γ)

Basic mechanism: formation of electromagnetic or hadronic showers.

Finally, the energy is converted into ionization or excitation of the matter.

Generic LHC Detector for all Particles

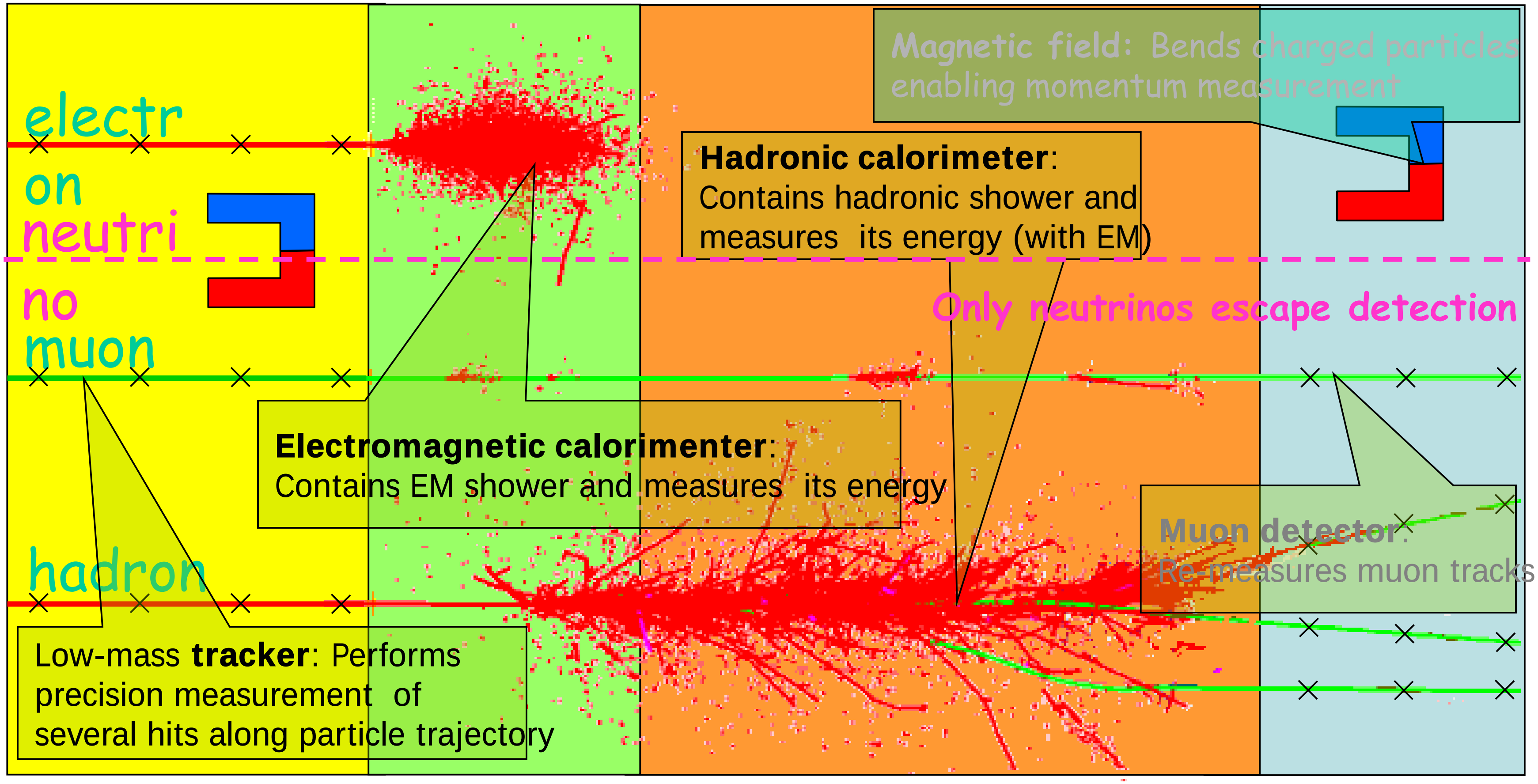

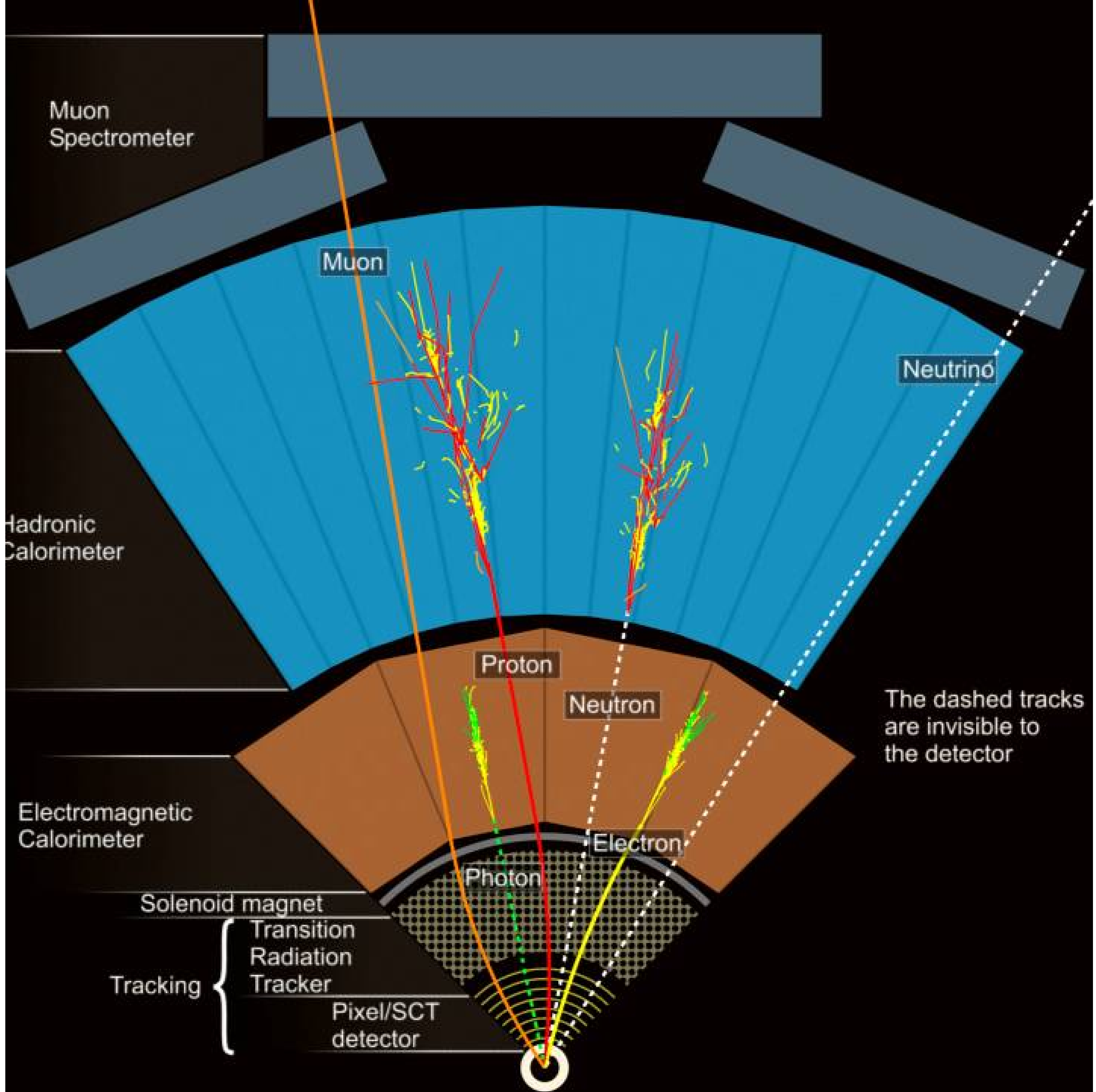

Muon Spectrometer
Muon
Neutrino
Hadronic Calorimeter
Proton
Neutron
The dashed tracks are invisible to the detector
Electromagnetic Calorimeter
Electron
Photon
Solenoid magnet
Transition Radiation Tracker
Tracking
Pixel/SCT detector

Mean energy loss by ionisation

Bethe-Bloch formula

For different materials

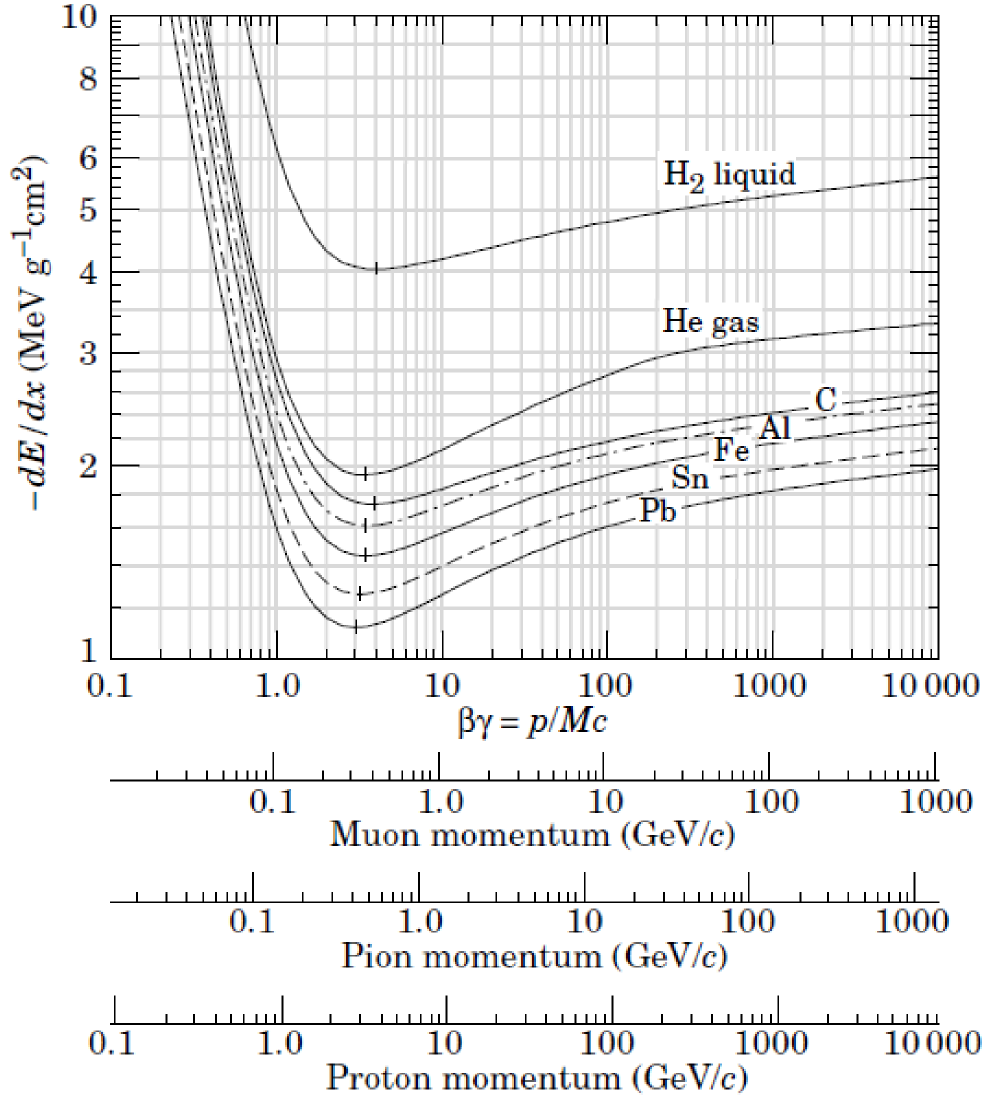

Figure 27.3: Mean energy loss rate in liquid (bubble chamber) hydrogen, gaseous helium, carbon, aluminum, iron, tin, and lead. Radiative effects, relevant for muons and pions, are not included. These become significant for muons in iron for $\beta\gamma \gtrsim 1000$, and at lower momenta for muons in higher-Z absorbers. See Fig. 27.21.

Energy loss by Bremsstrahlung

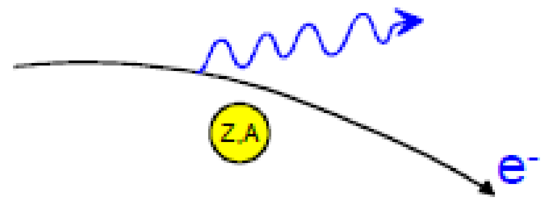

Radiation of real photons in the Coulomb field of the nuclei of the absorber

$$-\frac{dE}{dx} = 4\alpha N_A \frac{Z^2}{A} z^2 \left(\frac{1}{4\pi\varepsilon_0} \frac{e^2}{mc^2} \right)^2 E \ln\frac{183}{Z^{1/3}} \propto \frac{E}{m^2}$$

Effect plays a role only for $e^{\pm}$ and ultra-relativistic μ (>1000 GeV)

For electrons:

$$-\frac{dE}{dx} = 4\alpha N_A \frac{Z^2}{A} r_e^{\,2} E \ln\frac{183}{Z^{1/3}}$$

$$\boxed{-\frac{dE}{dx} = \frac{E}{X_0}}$$

$$X_0 = \frac{A}{4\alpha N_A Z^2 r_e^{\,2} \ln\frac{183}{Z^{1/3}}}$$

radiation length [g/cm²]

Material	Z	A	ρ [g/cm³]	X_0 [g/cm²]	λ_a [g/cm²]
Hydrogen (gas)	1	1.01	0.0899 (g/l)	63	50.8
Helium (gas)	2	4.00	0.1786 (g/l)	94	65.1
Beryllium	4	9.01	1.848	65.19	75.2
Carbon	6	12.01	2.265	43	86.3
Nitrogen (gas)	7	14.01	1.25 (g/l)	38	87.8
Oxygen (gas)	8	16.00	1.428 (g/l)	34	91.0
Aluminium	13	26.98	2.7	24	106.4
Silicon	14	28.09	2.33	22	106.0
Iron	26	55.85	7.87	13.9	131.9
Copper	29	63.55	8.96	12.9	134.9
Tungsten	74	183.85	19.3	6.8	185.0
Lead	82	207.19	11.35	6.4	194.0
Uranium	92	238.03	18.95	6.0	199.0

For Z > 6: $\lambda_a > X_0$

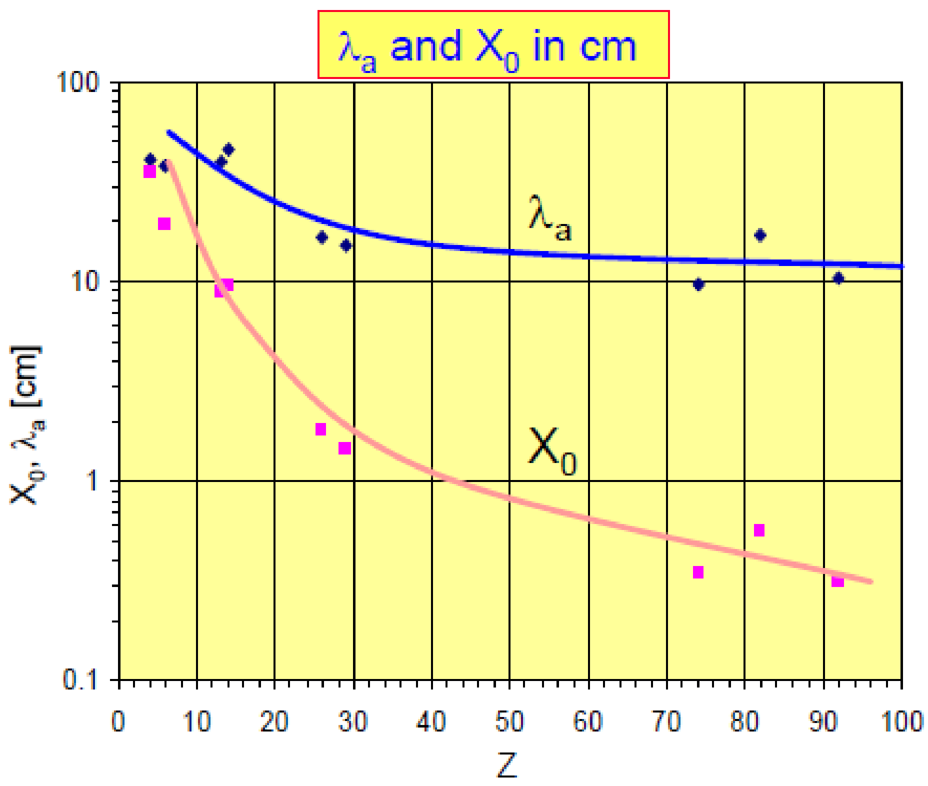

Electrons: fractional energy loss, 1/E dE/dx

Critical energy E_c

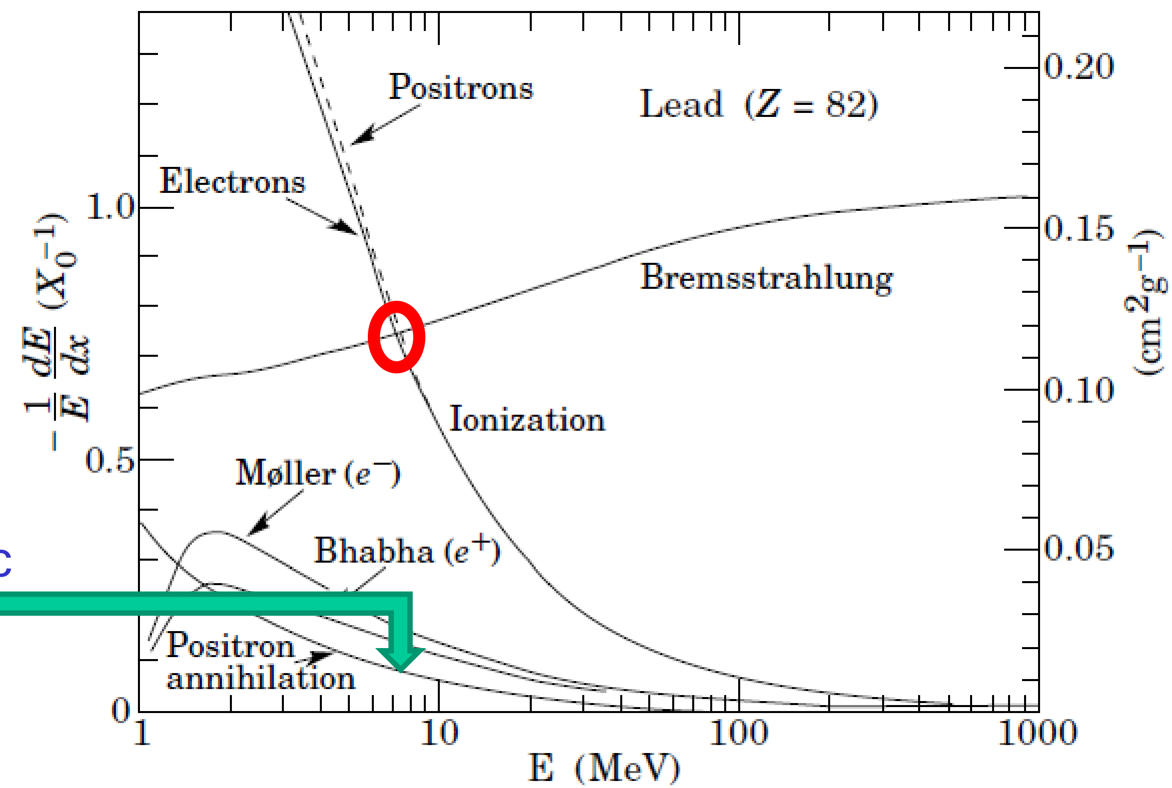

Figure 27.10: Fractional energy loss per radiation length in lead as a function of electron or positron energy. Electron (positron) scattering is considered as ionization when the energy loss per collision is below 0.255 MeV, and as Møller (Bhabha) scattering when it is above. Adapted from Fig. 3.2 from Messel and Crawford, *Electron-Photon Shower Distribution Function Tables for Lead, Copper, and Air Absorbers*, Pergamon Press, 1970. Messel and Crawford use $X_0(\mathrm{Pb}) = 5.82\ \mathrm{g/cm^2}$, but we have modified the figures to reflect the value given in the Table of Atomic and Nuclear Properties of Materials ($X_0(\mathrm{Pb}) = 6.37\ \mathrm{g/cm^2}$).

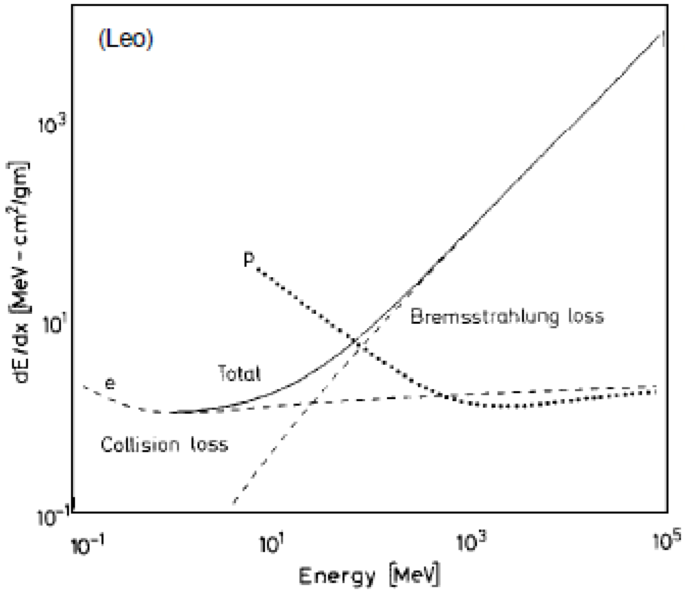

energy loss (radiative + ionization) of electrons and protons in copper

Critical energy E_c

$$\left.\frac{dE}{dx}(E_c)\right|_{Brems} = \left.\frac{dE}{dx}(E_c)\right|_{ion}$$

For electrons one finds approximately:

$$E_c^{solid+liq} = \frac{610 MeV}{Z+1.24} \qquad E_c^{gas} = \frac{710 MeV}{Z+1.24}$$

density effect of dE/dx(ionisation) !

$E_c(e^-)$ in Fe(Z=26) = 22.4 MeV

For muons

$$E_c \approx E_c^{elec}\left(\frac{m_\mu}{m_e}\right)^2$$

$E_c(\mu)$ in Fe(Z=26) $\approx$ 1 TeV

Interaction of photons with matter

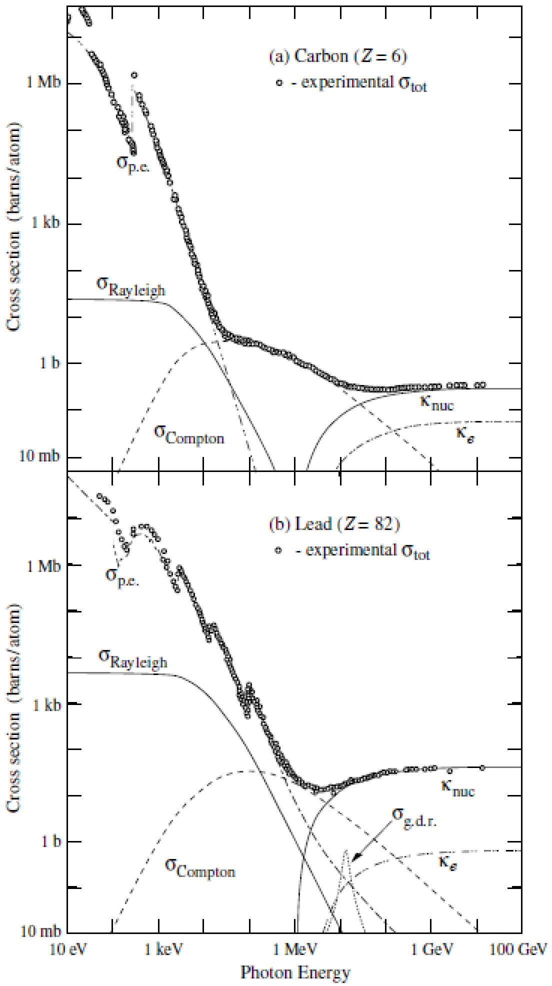

Figure 27.14: Photon total cross sections as a function of energy in carbon and lead, showing the contributions of different processes:

$\sigma_{\text{p.e.}}$ = Atomic photoelectric effect (electron ejection, photon absorption)

σ_{Rayleigh} = Rayleigh (coherent) scattering–atom neither ionized nor excited

σ_{Compton} = Incoherent scattering (Compton scattering off an electron)

κ_{nuc} = Pair production, nuclear field

κ_e = Pair production, electron field

$\sigma_{\text{g.d.r.}}$ = Photonuclear interactions, most notably the Giant Dipole Resonance [46]. In these interactions, the target nucleus is broken up.

Electromagnetic Cascades (showers)

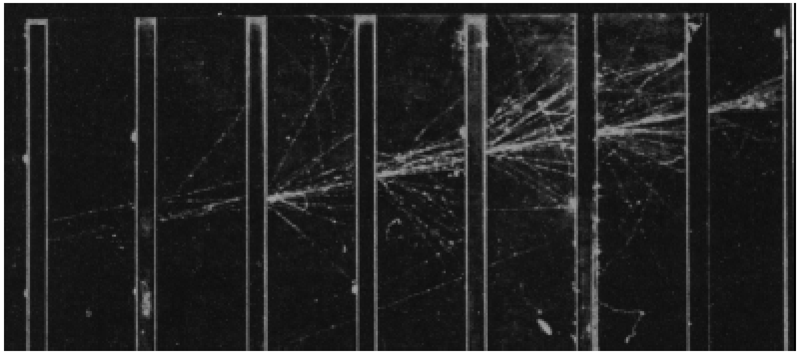

Electron shower in a cloud chamber with lead absorbers

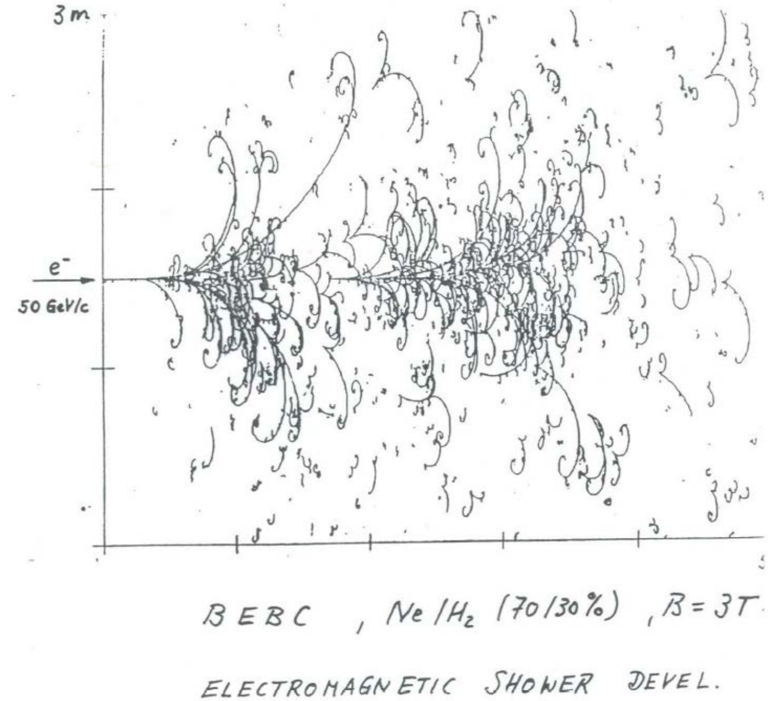

Simple qualitative model

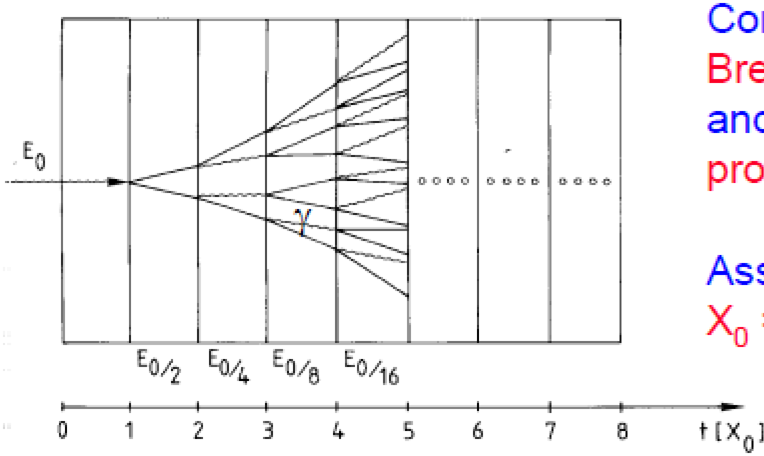

Consider only Bremsstrahlung and pair production.

Assume:
$X_0 = \lambda_{pair}$

$$N(t) = 2^t \qquad E(t)/\,particle = E_0 \cdot 2^{-t}$$

Process continues until $E(t) < E_c$

$$t_{\max} = \frac{\ln E_0/E_c}{\ln 2} \qquad N^{total} = \sum_{t=0}^{t_{\max}} 2^t = 2^{(t_{\max}+1)} - 1 \approx 2 \cdot 2^{t_{\max}} = 2\frac{E_0}{E_c}$$

After $t = t_{max}$ the dominating processes are ionization, Compton effect and photo effect → absorption.

→ Calorimeter size depends only logarithmically on E_0

Longitudinal shower development: $\frac{dE}{dt} \propto t^{\alpha} e^{-t}$

Detailed model: ″Rossi aproximaton B″

Shower maximum at $t_{\max} = \ln \frac{E_0}{E_c} \frac{1}{\ln 2}$

95% containment $t_{95\%} \approx t_{\max} + 0.08Z + 9.6$

Size of a calorimeter grows only logarithmically with E_0

Transverse shower development: 95% of the shower cone is located in a cylinder with radius 2 R_M

Determined mainly by multiple scattering of shower particles

$$R_M = \frac{21\,\mathrm{MeV}}{E_c} X_0 \quad [g/cm^2]$$ Molière radius

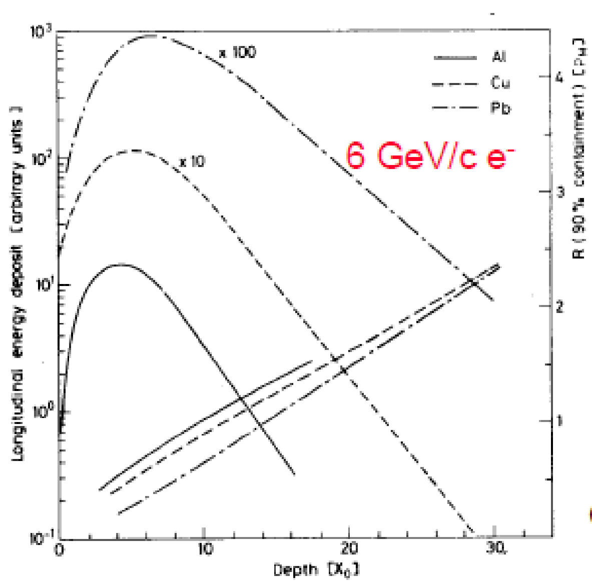

Longitudinal and transverse development scale with X_0, R_M

(C. Fabjan, T. Ludlam, CERN-EP/82-37)

Example: E_0 = 100 GeV in lead glass

E_c=11.8 MeV $\rightarrow t_{max} \approx 13$, $t_{95\%} \approx 23$

$X_0 \approx 2$ cm, $R_M = 1.8 \cdot X_0 \approx 3.6$ cm

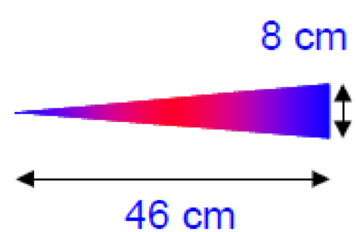

◆ Energy resolution of a calorimeter (intrinsic limit)

$$N^{total} \propto \frac{E_0}{E_c}$$ total number of track segments

$$\frac{\sigma(E)}{E} \propto \frac{\sigma(N)}{N} \propto \frac{1}{\sqrt{N}} \propto \frac{1}{\sqrt{E_0}}$$ holds also for hadron calorimeters

Also spatial and angular resolution scale like $1/\sqrt{E}$

Relative energy resolution of a calorimeter improves with E_0

More general:

$$\frac{\sigma(E)}{E} = \frac{a}{\sqrt{E}} \oplus b \oplus \frac{c}{E}$$

Stochastic term

Constant term

Inhomogenities
Bad cell inter-calibration
Non-linearities

Quality factor !

Noise term

Electronic noise
radioactivity
pile up

Calorimeter types

- **Homogeneous calorimeters:**
  - ⇨ Detector = absorber
  - ⇨ good energy resolution
  - ⇨ limited spatial resolution (particularly in longitudinal direction)
  - ⇨ only used for electromagnetic calorimetry

- **Sampling calorimeters:**
  - ⇨ Detectors and absorber separated $\rightarrow$ only part of the energy is sampled.
  - ⇨ limited energy resolution
  - ⇨ good spatial resolution
  - ⇨ used both for electromagnetic and hadron calorimetry

Homogeneous calorimeters

Two main types: Scintillator crystals or "glass" blocks (Cherenkov radiation).

→ photons. Readout via photomultiplier, -diode/triode

- Scintillators (crystals)

Scintillator	Density [g/cm³]	X_0 [cm]	Light Yield γ/MeV (rel. yield)	τ_1 [ns]	λ_1 [nm]	Rad. Dam. [Gy]	Comments
NaI (Tl)	3.67	2.59	4×10^4	230	415	≥10	hydroscopic, fragile
CsI (Tl)	4.51	1.86	5×10^4 (0.49)	1005	565	≥10	Slightly hygroscopic
CSI pure	4.51	1.86	4×10^4 (0.04)	10 36	310 310	10^3	Slightly hygroscopic
BaF_2	4.87	2.03	10^4 (0.13)	0.6 620	220 310	10^5	
BGO	7.13	1.13	8×10^3	300	480	10	
$PbW0_4$	8.28	0.89	≈100	10 10	≈440 ≈530	10^4	light yield =f(T)

Relative light yield: rel. to NaI(Tl) readout with PM (bialkali PC)

- Cherenkov radiators

Material	Density [g/cm³]	X_0 [cm]	n	Light yield [p.e./GeV] (rel. p.e.)	λ_{cut} [nm]	Rad. Dam. [Gy]	Comments
SF-5 Lead glass	4.08	2.54	1.67	600 (1.5×10^{-4})	350	10^2	
SF-6 Lead glass	5.20	1.69	1.81	900 (2.3×10^{-4})	350	10^2	
PbF_2	7.66	0.95	1.82	2000 (5×10^{-4})		10^3	Not available in quantity

Relative light yield: rel. to NaI(Tl) readout with PM (bialkali PC)

Examples

OPAL Barrel + end-cap: lead glass + pre-sampler

(OPAL collab. NIM A 305 (1991) 275)

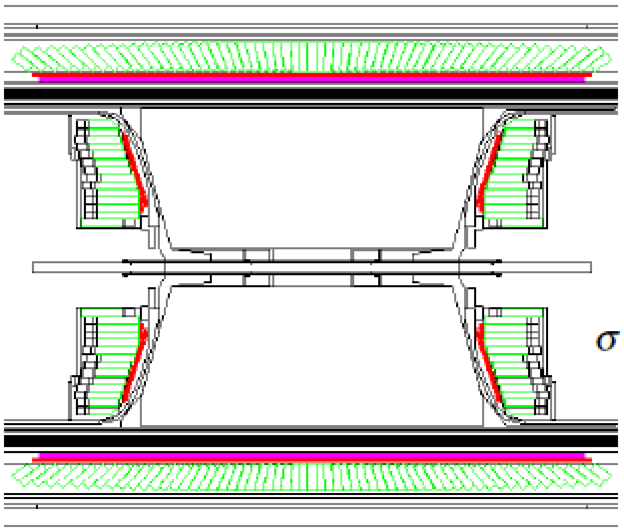

≈10500 blocks (10 x 10 x 37 cm^3, 24.6 X_0), PM (barrel) or PT (end-cap) readout.

$$\sigma(E)/E = 0.06/\sqrt{E} \oplus 0.002$$

Spatial resolution (intrinsic) ≈ 11 mm at 6 GeV

BGO E.M. Calorimeter in L3

(L3 collab. NIM A 289 (1991) 53)

11000 crystals, 21.4 X_0,
temperature monitoring + control system
light output -1.55% / °C

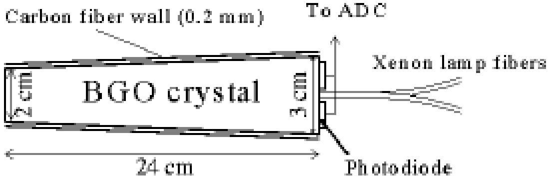

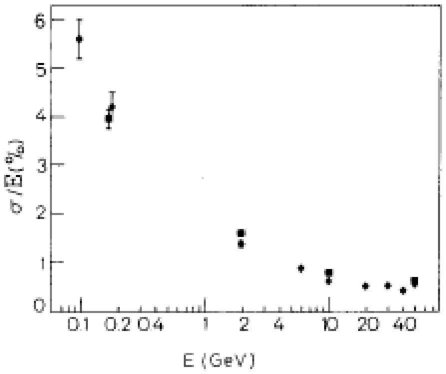

σ_E/E < 1% for E > 1 GeV
spatial resolution < 2 mm
(E >2 GeV)

Partly test beam results !

NA48: LKr Ionisation chamber (T = 120 K)

no metal absorbers → quasi homogenous !

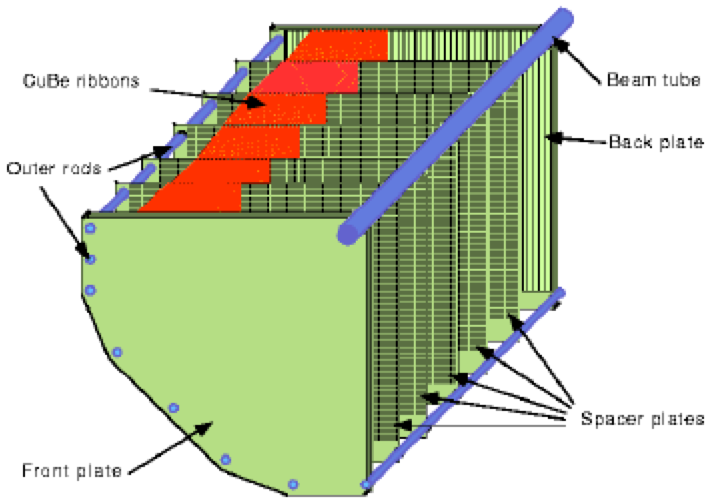

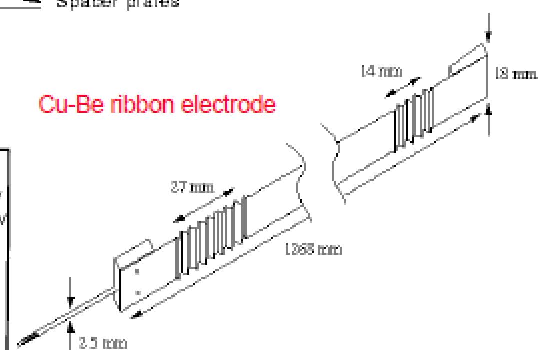

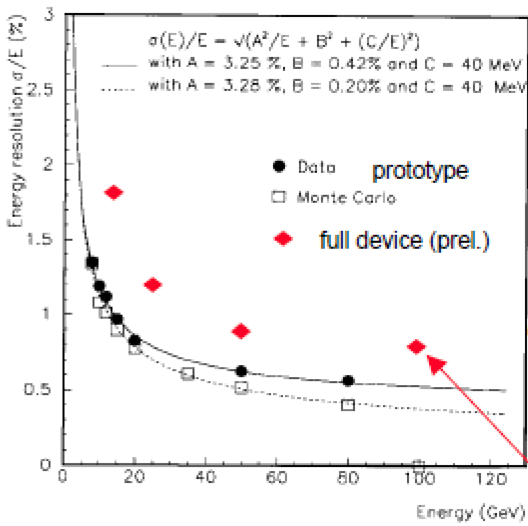

$\sigma_{x,y} \leq 1$ mm

$\sigma_t \approx 230$ ps

97 run: reduced performance due to problems with blocking capacitors → lower driftfield: 1.5 kV/cm rather than 5 kV/cm

(V. Marzulli, NIM A 384 (1996) 237,
M. Martini et al., VII International Conference on Calorimetry, Tuscon, 1997)

Sampling calorimeters

Absorber + detector separated $\rightarrow$ additional sampling fluctuations

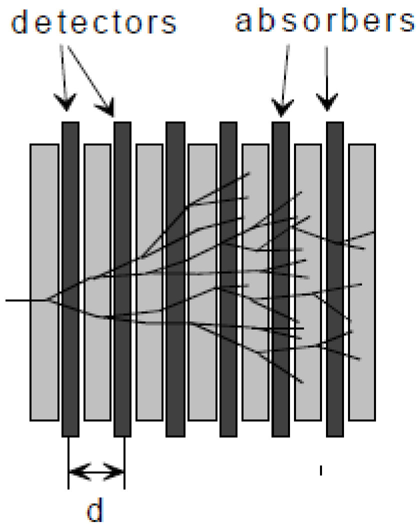

$$N = \frac{T_{\det}}{d}$$ Detectable track segments

$$= F(\xi)\frac{E}{E_c}X_0\frac{1}{d}$$

$$\frac{\sigma(E)}{E} \propto \frac{\sqrt{N}}{N} \propto \sqrt{\frac{1}{E}} \cdot \sqrt{\frac{d}{X_0}}$$

- MWPC, streamer tubes
- warm liquids
  TMP = tetramethylpentane,
  TMS = tetramethylsilane
- cryogenic noble gases:
  mainly LAr (Lxe, LKr)
- scintillators, scintillation fibres, silicon detectors

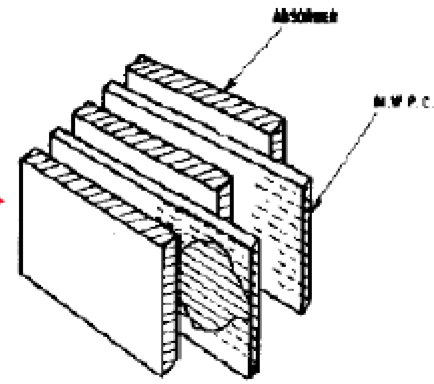

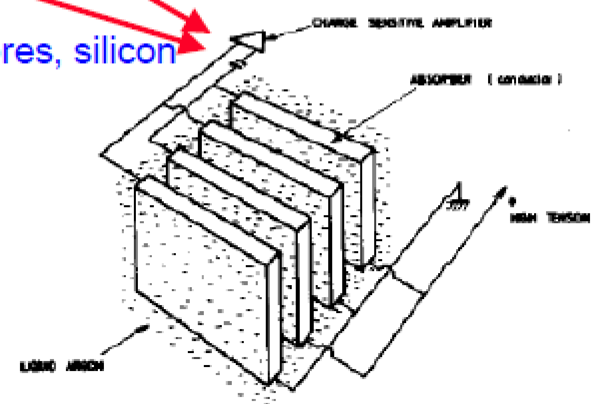

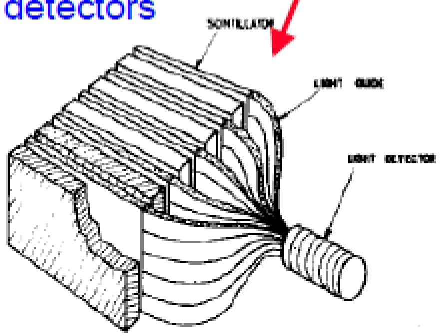

◆ ATLAS electromagnetic Calorimeter

Accordion geometry absorbers immersed in Liquid Argon

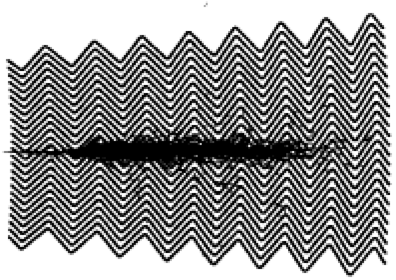

(RD3 / ATLAS)

Liquid Argon (90K)

+ lead-steal absorbers (1-2 mm)

+ multilayer copper-polyimide readout boards

→ Ionization chamber.

1 GeV E-deposit → 5 x10^6 e^-

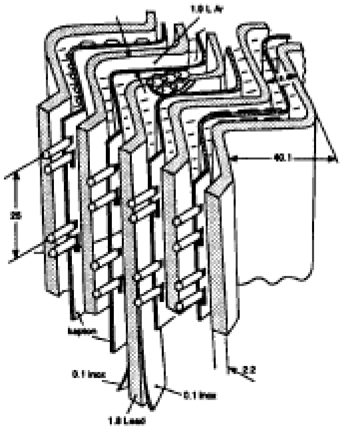

- Accordion geometry minimizes dead zones.
- Liquid Ar is intrinsically radiation hard.
- Readout board allows fine segmentation (azimuth, pseudo-rapidity and longitudinal) acc. to physics needs

Test beam results, e^- 300 GeV (ATLAS TDR)

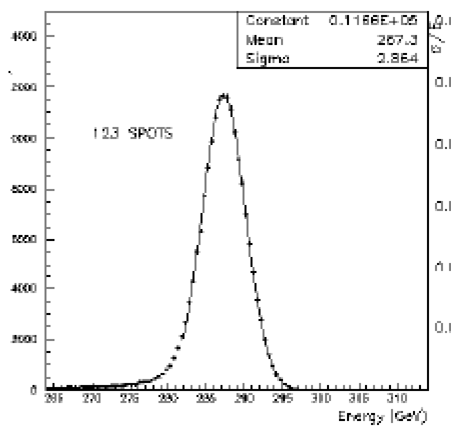

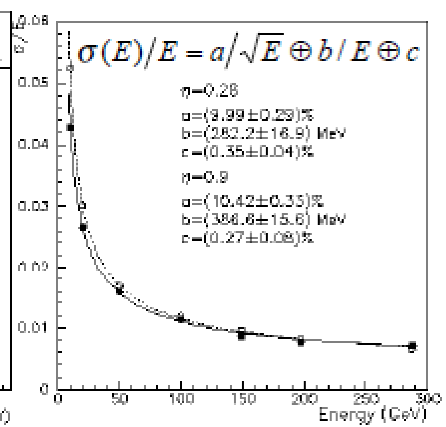

Spatial and angular uniformity ≈0.5%

Spatial resolution ≈ 5mm / $E^{1/2}$

Material in front of calorimeter

Showers start in 'dead' material in front of calorimeter (other detectors, solenoid, support structure)

Install a highly segmented pre-shower detector in front of calorimeter

- recover lost energy
- improved background rejection due to good spatial resolution
- improve angular resolution

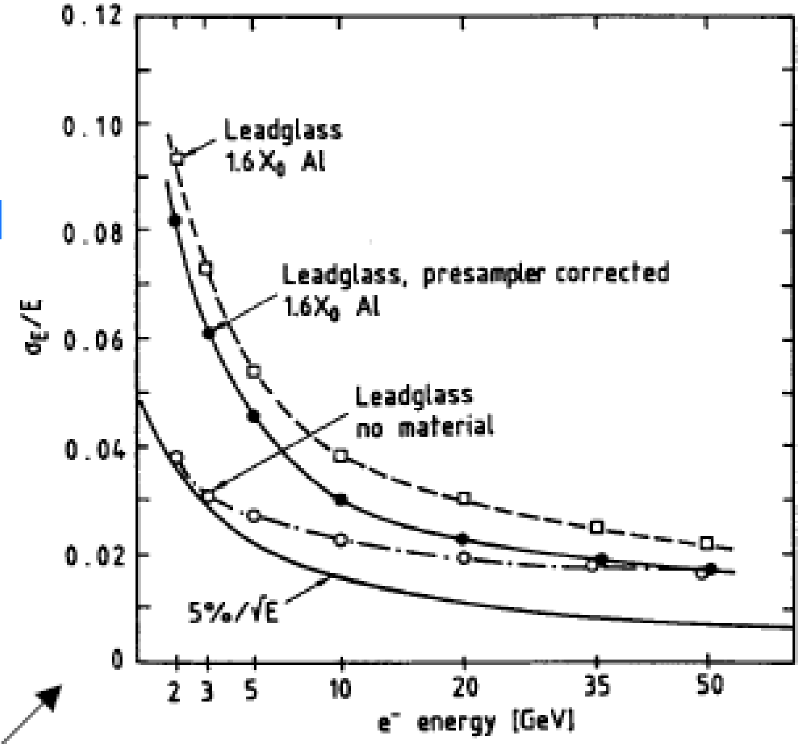

(C. Beard et al., NIM A 286 (1990) 117)

OPAL end cap calorimeter + pre-shower

Nuclear Interactions

The interaction of energetic hadrons (charged or neutral) is determined by inelastic nuclear processes.

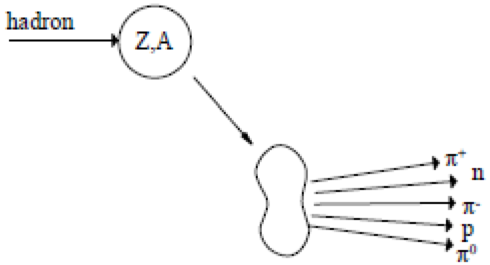

multiplicity $\propto \ln(E)$

$p_t \approx 0.35$ GeV/c

Excitation and finally breakup up nucleus $\rightarrow$ nucleus fragments + production of secondary particles.

For high energies (>1 GeV) the cross-sections depend only little on the energy and on the type of the incident particle (p, π, K…).

$$\sigma_{inel} \approx \sigma_0 A^{0.7} \quad \sigma_0 \approx 35\, mb$$

In analogy to X_0 a hadronic absorption length can be defined

$$\lambda_a = \frac{A}{N_A \sigma_{inel}} \propto A^{\frac{1}{4}} \quad \text{because } \sigma_{inel} \approx \sigma_0 A^{0.7}$$

similarly a hadronic interaction length

$$\lambda_I = \frac{A}{N_A \sigma_{total}} \propto A^{\frac{1}{3}} \qquad \lambda_I < \lambda_a$$

Material	Z	A	ρ [g/cm³]	X_0 [g/cm²]	λ_a [g/cm²]
Hydrogen (gas)	1	1.01	0.0899 (g/l)	63	50.8
Helium (gas)	2	4.00	0.1786 (g/l)	94	65.1
Beryllium	4	9.01	1.848	65.19	75.2
Carbon	6	12.01	2.265	43	86.3
Nitrogen (gas)	7	14.01	1.25 (g/l)	38	87.8
Oxygen (gas)	8	16.00	1.428 (g/l)	34	91.0
Aluminium	13	26.98	2.7	24	106.4
Silicon	14	28.09	2.33	22	106.0
Iron	26	55.85	7.87	13.9	131.9
Copper	29	63.55	8.96	12.9	134.9
Tungsten	74	183.85	19.3	6.8	185.0
Lead	82	207.19	11.35	6.4	194.0
Uranium	92	238.03	18.95	6.0	199.0

For $Z > 6$: $\lambda_a > X_0$

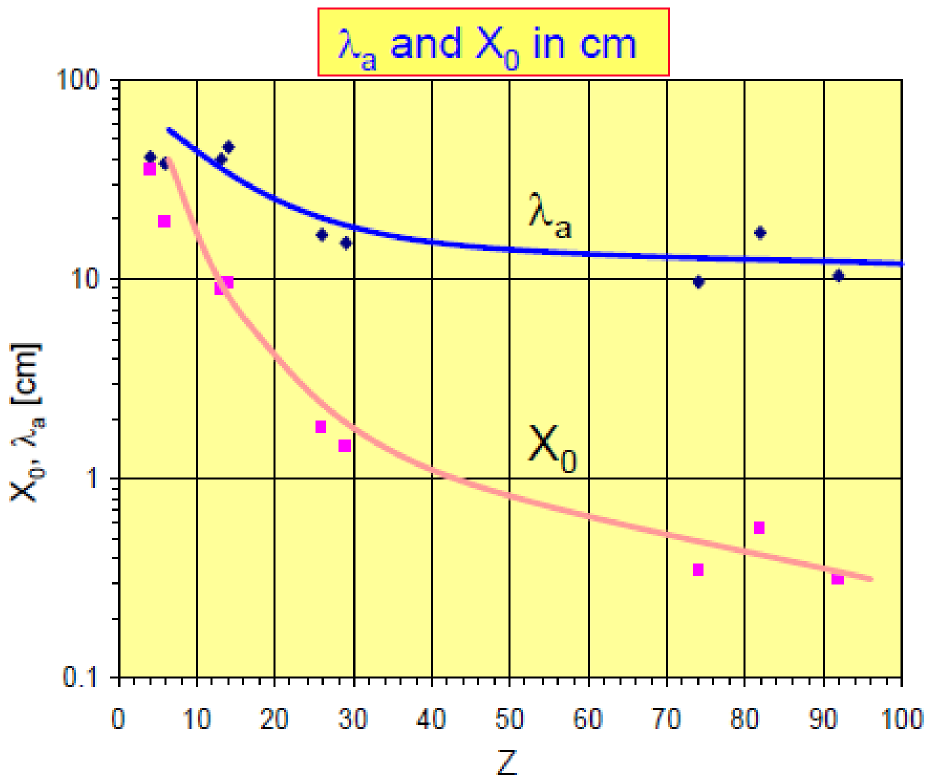

Interaction of neutrons

Neutrons have no charge, i.e. their interaction is based only on strong (and weak) nuclear force.

To detect neutrons, we have to create charged particles.

Possible neutron conversion and elastic reactions

- $n + {}^{6}Li \rightarrow \alpha + {}^{3}H$
- $n + {}^{10}B \rightarrow \alpha + {}^{7}Li$
- $n + {}^{3}He \rightarrow p + {}^{3}H$

$E_n < 20$ MeV

- $n + p \rightarrow n + p$ $\quad E_n < 1$ GeV

(H. Neuert, Kernphysikalische Messverfahren, G. Braun Verlag, 1966)

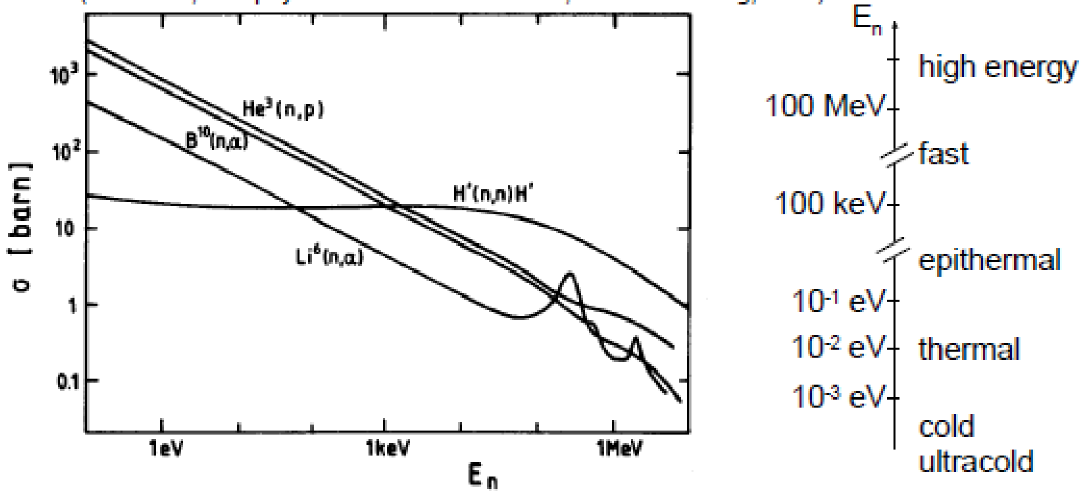

In addition there are

- neutron induced fission $\quad E_n \approx E_{th} \approx \frac{1}{40}\,\text{eV}$
- hadronic cascades (see below) $\quad E_n > 1$ GeV

Hadronic casacdes

Various processes involved. Much more complex than electromagnetic cascades.

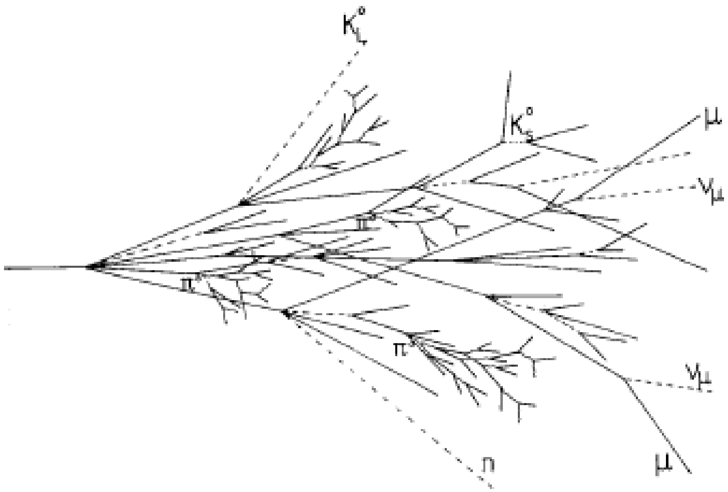

(Grupen)

Hadronic + electromagnetic component

↓

charged pions, protons, kaons ….
Breaking up of nuclei
(binding energy),
neutrons, neutrinos, soft γ's
muons …. → invisible energy

↓

neutral pions → 2γ →
electromagnetic cascade

$$n(\pi^0) \approx \ln E(GeV) - 4.6$$

example 100 GeV: $n(\pi^0) \approx 18$

Large energy fluctuations → limited energy resolution

Longitudinal shower development

$$t_{\max}(\lambda_I) \approx 0.2 \ln E[GeV] + 0.7$$

$$t_{95\%} \approx a \ln E + b$$

For Iron: a = 9.4, b=39
E =100 GeV
$\rightarrow t_{95\%} \approx 80$ cm

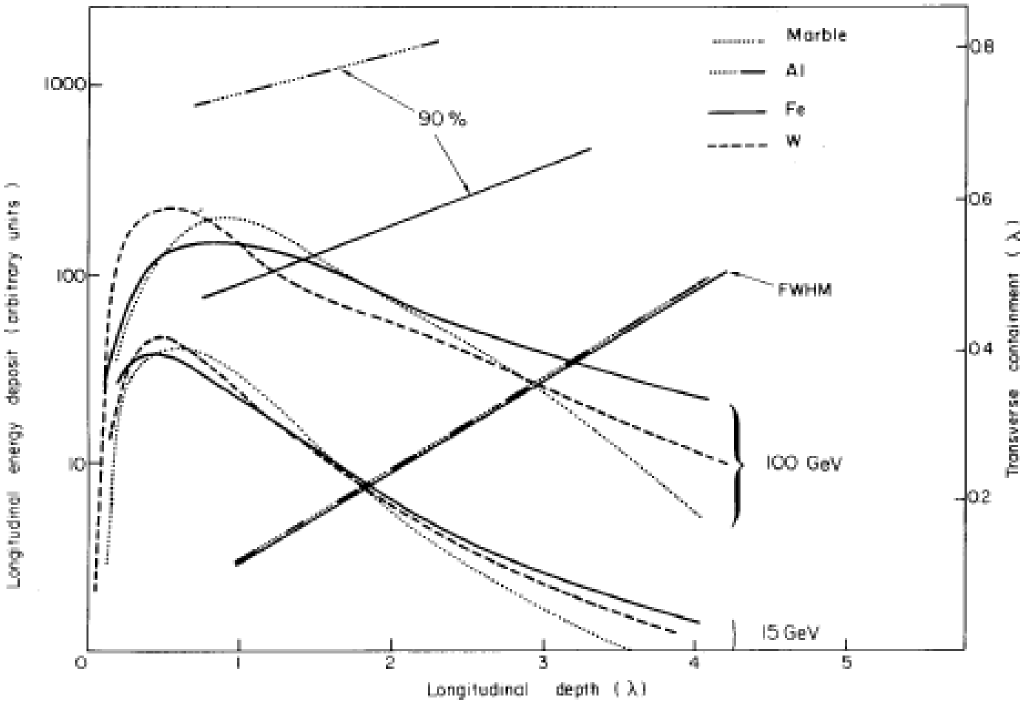

(C. Fabjan, T. Ludlam, CERN-EP/82-37)

→ Hadronic showers are much longer and broader than electromagnetic ones!

Laterally shower consists of core + halo. 95% containment in a cylinder of radius λ_I.

Iron: λ_I=16.7 cm

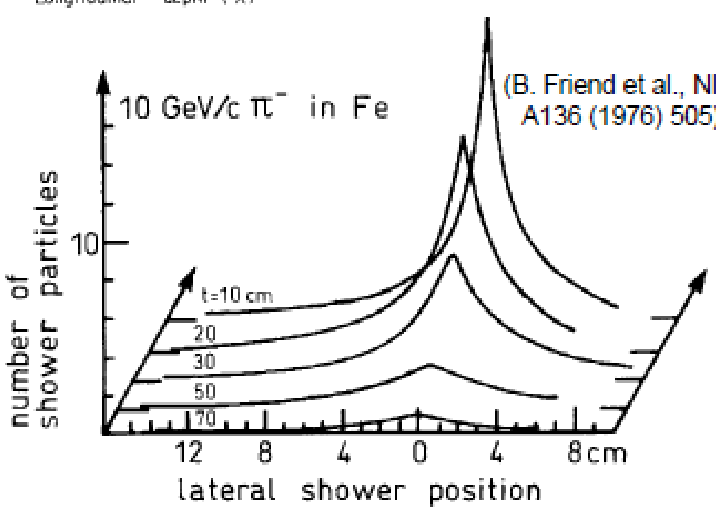

(B. Friend et al., NIM A136 (1976) 505)

◆ CMS Hadron calorimter

Cu absorber + scintillators

↓

2 x 18 wedges (barrel)

+ 2 x 18 wedges (endcap) ≈ 1500 T absorber

Scintillators fill slots and are read out via fibres by HPDs

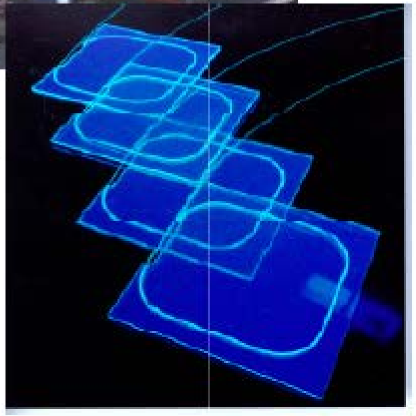

Test beam resolution for single hadrons

$$\frac{\sigma_E}{E} = \frac{65\%}{\sqrt{E}} \oplus 5\%$$

4 scintillating tiles of the CMS Hadron calorimeter

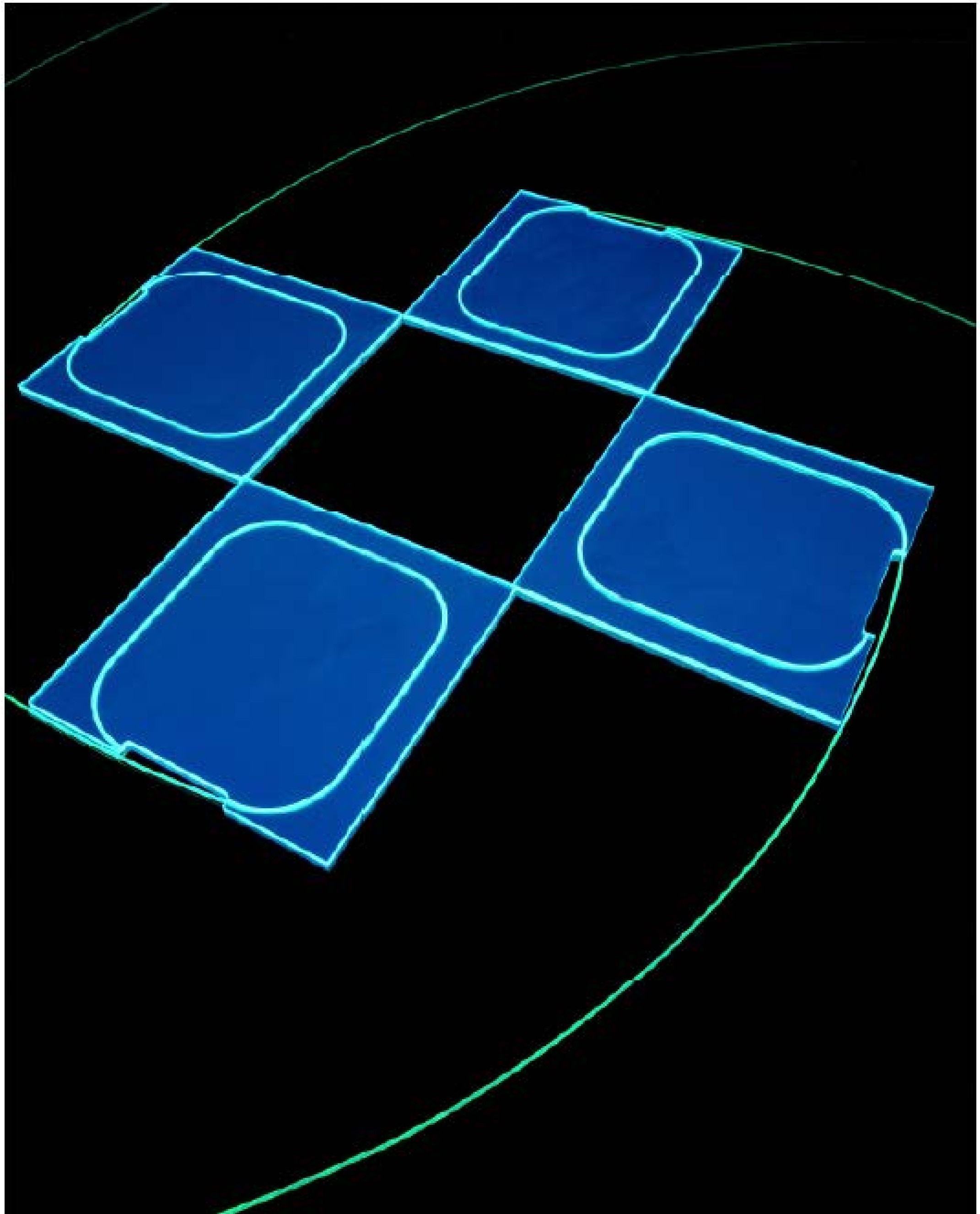

Atmosphere as a calorimeter

Need:

- detect high energy cosmic rays
- Measure their energy
- Determine the identity (gamma or hadron, which hadron)

Idea: use atmosphere as a detector + calorimeter

Virtues:

- A lot of material
- Transparent

Use Cherenkov light emitted by charged particles to determine the energy of the incoming cosmic ray.

Detection of high-energy gamma rays

using Cherenkov telescopes

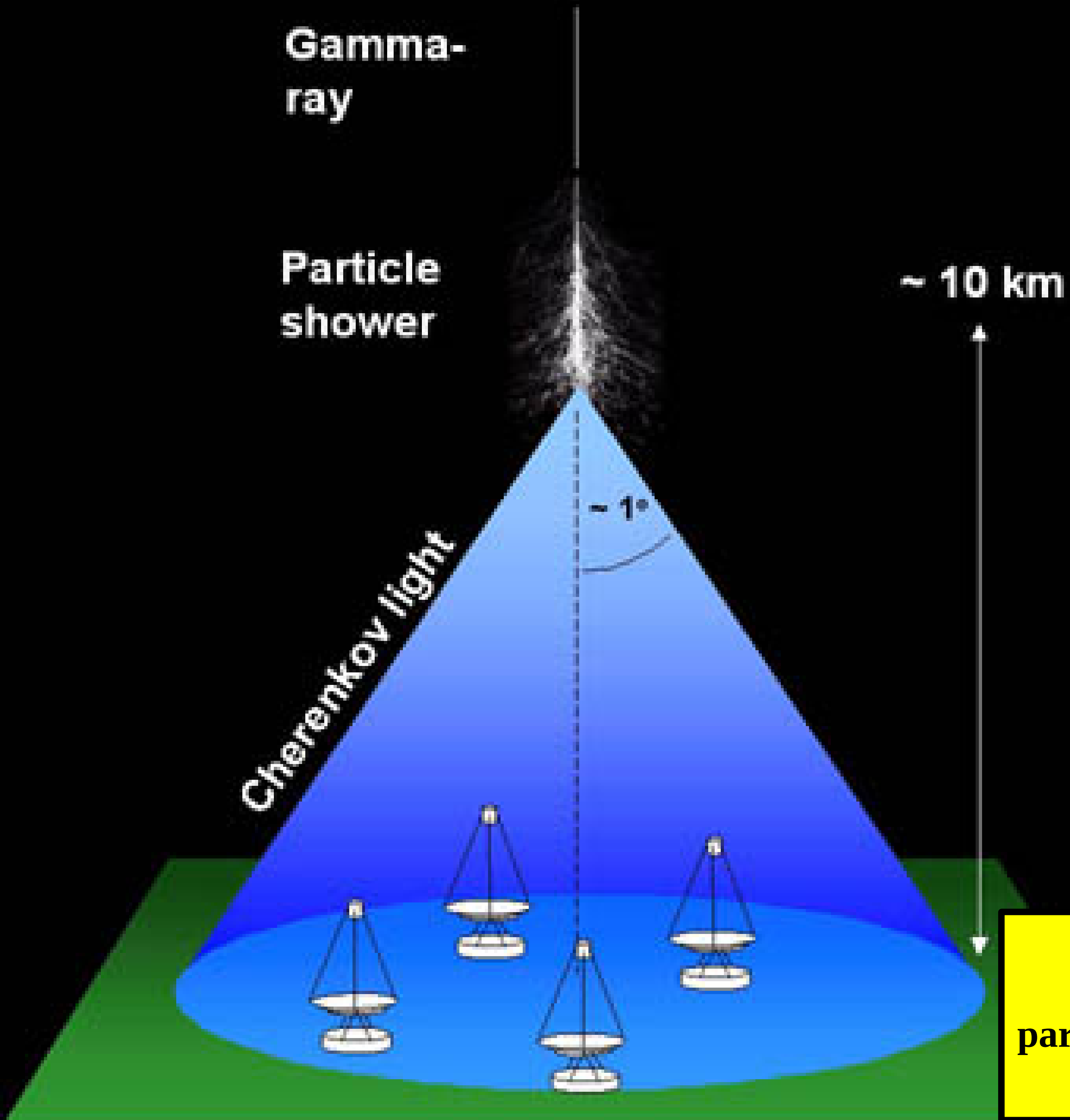

Shower mainly E-M. Thousands of relativistic particles give Čerenkov light in upper atmosphere

HESS 1 UHE Gamma Ray Telescope Stereoscopic Quartet

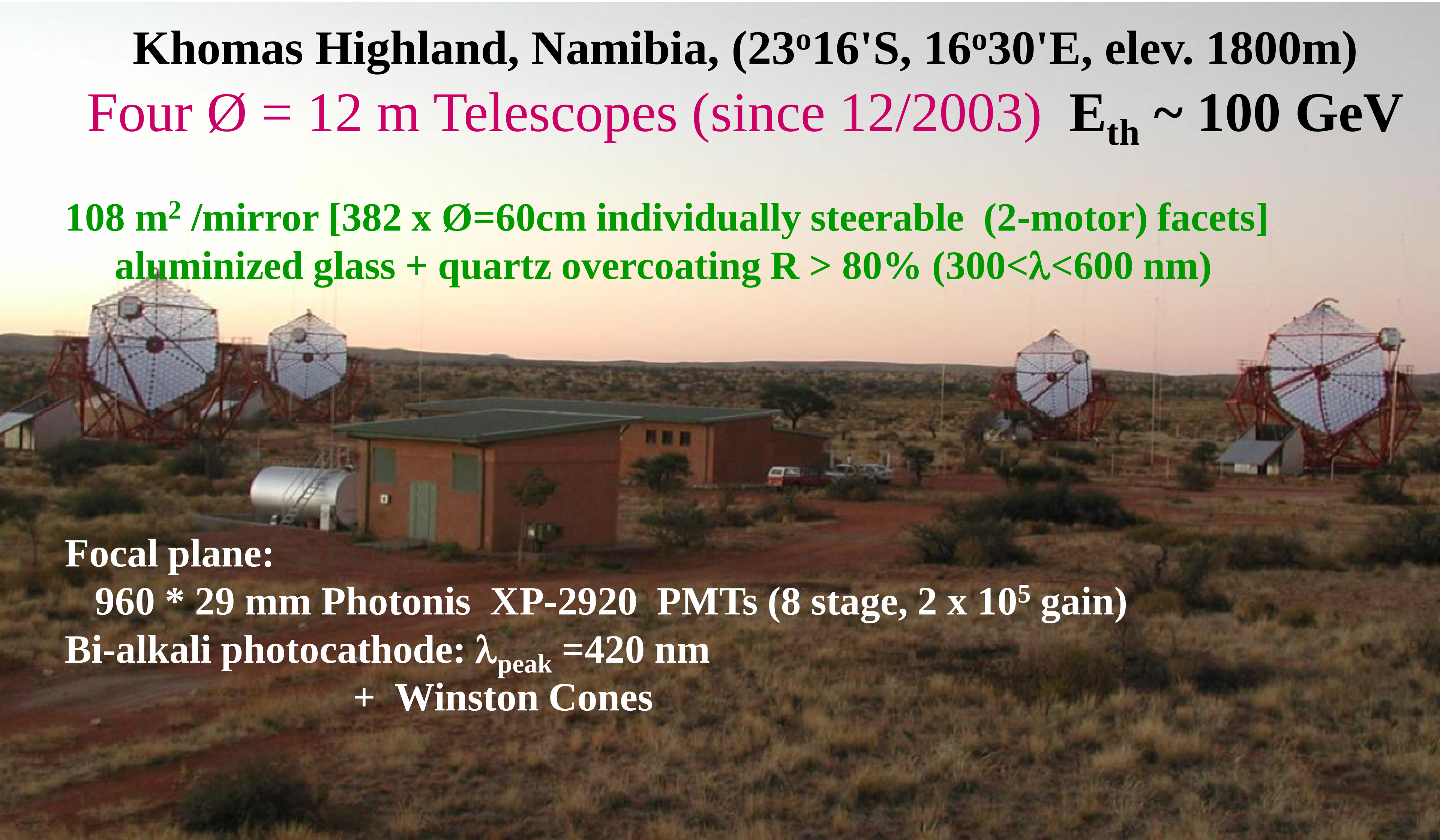

Khomas Highland, Namibia, (23º16'S, 16º30'E, elev. 1800m)

Four Ø = 12 m Telescopes (since 12/2003) **E_{th} ~ 100 GeV**

108 m^2 /mirror [382 x Ø=60cm individually steerable (2-motor) facets]
aluminized glass + quartz overcoating R > 80% (300<λ<600 nm)

Focal plane:
960 * 29 mm Photonis XP-2920 PMTs (8 stage, 2 x 10^5 gain)
Bi-alkali photocathode: λ_{peak} =420 nm
+ Winston Cones

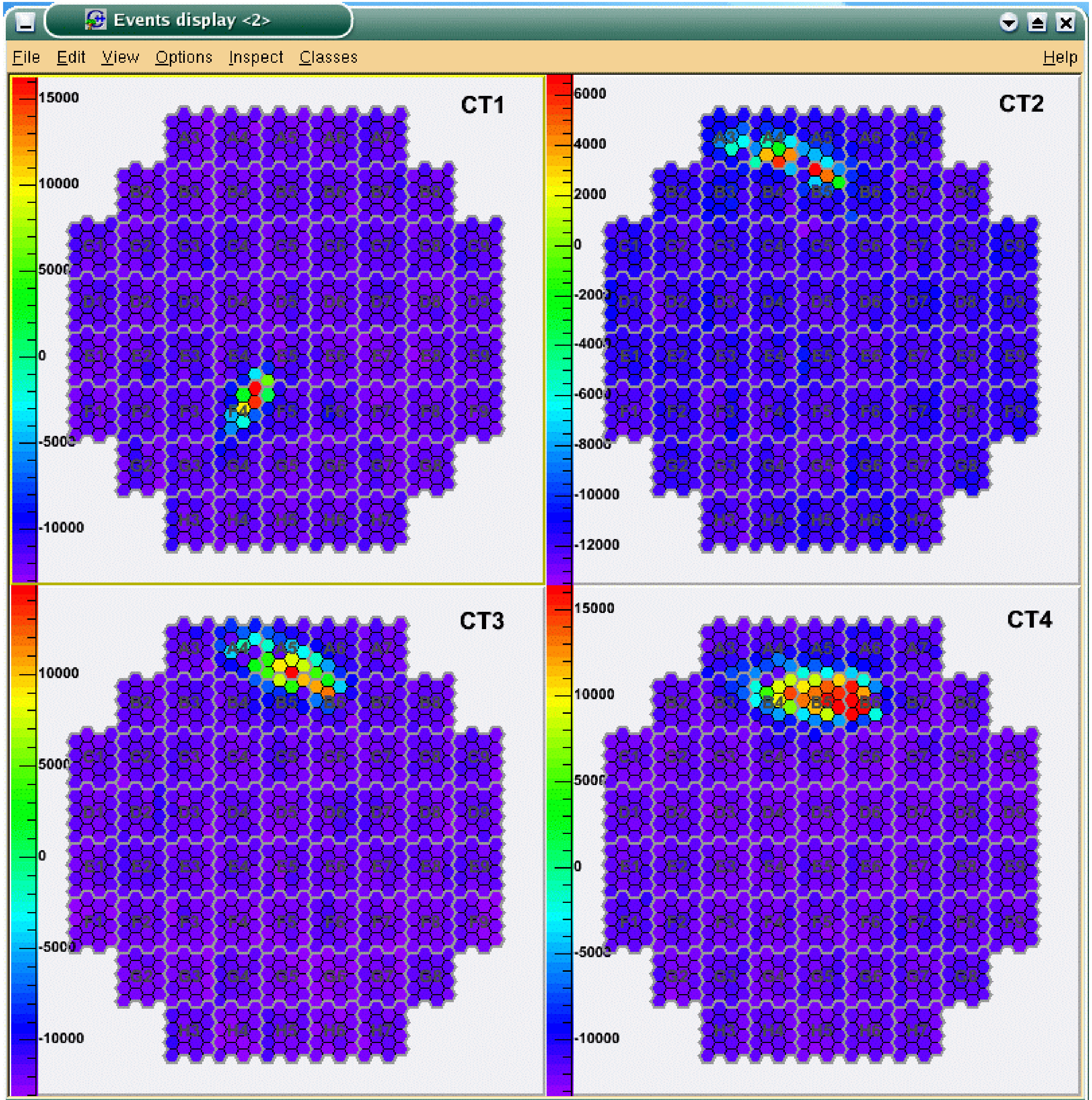

Events display <2>
File
Edit
View
Options
Inspect
Classes
Help
CT1
15000
10000
5000
0
-5000
-10000
CT2
6000
4000
2000
0
-2000
-4000
-6000
-8000
-10000
-12000
CT3
10000
5000
0
-5000
-10000
CT4
15000
10000
5000
0
-5000
-10000